Title

Nanoparticulate Mineralized Collagen Scaffolds and BMP-9 Induce a Long-Term Bone Cartilage Construct in Human Mesenchymal Stem Cells

Journal

Advanced Healthcare Materials, 5(14)

ISSN

2192-2640

Authors

Ren, Xiaoyan
Weisgerber, Daniel W
Bischoff, David
et al.

Publication Date

2016-07-01

DOI

10.1002/adhm.201600187

Peer reviewed

Published in final edited form as:
Adv Healthc Mater. 2016 July ; 5(14): 1821–1830. doi:10.1002/adhm.201600187.

Nanoparticulate Mineralized Collagen Scaffolds and BMP-9 Induce a Long Term Bone Cartilage Construct in Human Mesenchymal Stem Cells

Xiaoyan Ren, MD, PhD[1,2], **Daniel W. Weisgerber, BA**[3], **David Bischoff, PhD**[2], **Michael S. Lewis, MD, PhD**[4], **Russell R. Reid, MD, PhD**[5], **Tong-chuan He, MD, PhD**[6], **Dean T. Yamaguchi, MD, PhD**[2], **Timothy A. Miller, MD**[1,2], **Brendan A.C. Harley, ScD**[3], and **Justine C. Lee, MD, PhD**[1,2,*]

[1]Division of Plastic and Reconstructive Surgery, UCLA David Geffen School of Medicine, Los Angeles, CA 90095

[2]Research Service, Greater Los Angeles VA Healthcare System, Los Angeles, CA 90073

[3]Department of Chemical and Biomolecular Engineering, Institute for Genomic Biology, University of Illinois at Urbana-Champaign, Urbana, IL 61801

[4]Department of Pathology, Greater Los Angeles VA Healthcare System, Los Angeles, CA 90073

[5]Section of Plastic and Reconstructive Surgery, University of Chicago, IL 60637

[6]Department of Orthopaedic Surgery, University of Chicago, Chicago, IL 60637

Abstract

Engineering the osteochondral junction requires fabrication of a microenvironment that supports both osteogenesis and chondrogenesis. Multiphasic scaffold strategies utilizing a combination of soluble factors and extracellular matrix components are ideally suited for such applications. In this work, we evaluated the contribution of an osteogenic nanoparticulate mineralized glycosaminoglycan scaffold (MC-GAG) and a dually chondrogenic and osteogenic growth factor, BMP-9, in the differentiation of primary human mesenchymal stem cells (hMSCs). Although two dimensional cultures demonstrated alkaline phosphatase activity and mineralization of hMSCs induced by BMP-9, MC-GAG scaffolds did not demonstrate significant differences in collagen I expression, osteopontin expression, or mineralization. Instead, BMP-9 increased expression of collagen II, Sox9, aggrecan (ACAN), and cartilage oligomeric protein (COMP). However, the hypertrophic chondrocyte marker, collagen X, was not elevated with BMP-9 treatment. In addition, histologic analyses demonstrated that while BMP-9 did not increase mineralization, BMP-9 treatment resulted in an increase of sulfated glycosaminoglycans. Thus, the combination of BMP-9 and MC-GAG stimulated chondrocytic and osteogenic differentiation of hMSCs.

[*]Corresponding Author: Justine C. Lee, MD, PhD, UCLA Division of Plastic and Reconstructive Surgery, 200 UCLA Medical Plaza, Suite 465, Los Angeles, CA 90095, justine@ucla.edu, Phone: (310) 794-7616, Fax: (310) 206-6833.

Disclosures: The authors have no disclosures.

Keywords

osteochondral regeneration; biomimetic material; nanoparticulate mineralization; BMP9

Introduction

Diseases of the joint are debilitating afflictions that affect both the axial and craniofacial skeleton. Although a multitude of surgical techniques have been described for joint reconstruction, significant morbidity, recurrence, and reoperation highlight the need for alternative means of treatment such as regenerative technology. Unlike bone or cartilage alone, articular joints pose a special problem in tissue engineering in that simple tissues must be united into a multilayer, stable configuration. Specifically, the osteochondral junction is a stratified unit containing non-calcified cartilage, calcified cartilage, and the subchondral bone [1]. Fabrication of the osteochondral junction requires identification of methods for stable maintenance of different cell types and a blended, continuous interface between mechanically different tissue components.

The bone morphogenetic protein (BMP) superfamily of growth factors has been utilized to instruct osteogenesis and chondrogenesis in both bone marrow and adipose derived stem cells [2]. BMP-9, a lesser known member of the BMP family, was recently shown to be the most osteogenic BMP in both *in vitro* and *in vivo* studies using primary and immortalized multipotent cells from multiple species [3–6]. Function and intracellular signaling pathways differ somewhat between BMP-9 and other osteogenic BMPs, such as BMP-2. While both activated endochondral ossification via the receptor Smads (Smad1/5/8), the non-canonical, Smad1/5-independent pathway is thought to be a necessary element in BMP-9 signalling [5, 7–9]. Interestingly, BMP-9 also has a role in chondrogenic differentiation of mesenchymal stem cells and induction of chondrocytic hypertrophy [10]. In primary human mesenchymal stem cells, Majumdar and colleagues demonstrated that both BMP-2 and BMP-9 upregulated gene expression of three cartilage-specific genes: Sox-9 transcription factor, a 79 amino acid high mobility group type DNA binding protein with high homology to sex-determining region Y (Sry), type II collagen (Col2A1), and the proteoglycan aggrecan (ACAN) [11]. Of note, BMP-9 was uniformly more effective than BMP-2 at inducing expression of cartilage genes at the same dosage. Thus, BMP-9 is potentially both the most osteogenic and the most chondrogenic bone morphogenetic protein in pluripotent cell types [12]. This duality in function may be harnessed in tissue engineering strategies especially in combination tissues such as the osteochondral junction.

Decisions for lineage commitment to osteogenesis versus chondrogenesis require the proper combination of growth factors and other cues such as the extracellular matrix and mechanical loading [13]. Thus, regenerative strategies that incorporate multiple elements may allow for fine tuned modulation of cellular differentiation. We recently reported that crosslinking and addition of nanoparticulate mineral content to collagen glycosaminoglycan scaffolds (MC-GAG) resulted in higher biomimicry, osteogenic capabilities, and structural stability [14]. In addition, both primary human mesenchymal stem cells (hMSCs) and primary rabbit bone marrow stromal cells (rBMSCs) underwent osteogenic differentiation

on MC-GAG scaffolds in a manner that surpassed non-mineralized scaffolds and in the absence of exogenous BMP-2 stimulation [15]. In this work, we evaluate the effects of BMP-9 on primary human mesenchymal stem cells on MC-GAG scaffolds. Specifically, we seek to establish a stable bone cartilage construct to recapitulate the osteochondral junction.

Materials and Methods

Fabrication and crosslinking of mineralized collagen scaffolds

MC-GAG scaffolds were prepared using the lyophilization process described previously [16, 17]. Briefly, a collagen-glycosaminoglycan-calcium phosphate (CGCaP) suspension was produced by combining microfibrillar, type I collagen (Collagen Matrix, Oakland, NJ) and chondroitin-6-sulfate (Sigma-Aldrich, St. Louis, MO) in a solution of 0.05 M acetic acid (pH 3.2) or with calcium salts (calcium nitrate hydrate: $Ca(NO_3)_2{\cdot}4H_2O$; calcium hydroxide: $Ca(OH)_2$, Sigma-Aldrich) in a solution of phosphoric acid, respectively. The suspension was frozen using a constant cooling rate technique (1°C/min) from room temperature to a final freezing temperature of −10°C and sublimated under vacuum (<200 mTorr, 0°C). Disks 8 mm in diameter were prepared using punch biopsies for cultures and sterilized via ethylene oxide. Scaffolds were rehydrated with phosphate buffered saline (PBS, Sigma Aldrich) and crosslinked in a solution of 1-ethyl-3-(3-dimethylaminopropyl) carbodiimide (EDC, Sigma Aldrich) and N-hydroxysuccinimide (NHS, Sigma Aldrich) at a molar ratio of 5:2:1 EDC:NHS:COOH [18]. The concentrations of EDC and NHS employed for crosslinking the scaffolds were 0.0111 g/scaffold EDC and 0.0026 g/scaffold NHS, based on previously established methods [19, 20]. After crosslinking, the scaffolds were washed in fresh PBS for an additional 2 h to remove any remaining chemical.

Adenoviral Transduction of human mesenchymal stem cells

2D: hMSCs ($CD105^+CD166^+CD29^+CD44^+CD14^-CD34^-CD45^-$) from a bone marrow source (Lonza, Inc., Allendale, NJ) were expanded in DMEM supplemented with 10% fetal bovine serum (Atlanta Biologicals, Atlanta, GA), 2 mM L-glutamine (Life Technologies, Carlsbad, CA), 100 IU/ml penicillin/100 μg/ml streptomycin (Life Technologies). At passage 3, hMSCs were plated at 5000 – 10,000 cells per well in 12 and 6-well plates respectively, grown until 80% confluent, and then transduced with an adenovirus expressing BMP-9 and GFP (AdBMP-9) in DMEM at a multiplicity of infection (MOI) of 100 and 8μg/ml of polybrene (Sigma-Aldrich, St. Louis, MO). 24 hours after transduction, hMSCs were subjected to differentiation medium consisting of 10 mM β-glycerophosphate, 50 μg/ml ascorbic acid and 0.1μM dexamethasone. Cell cultures were evaluated on days 7, 14 and 21 post-transduction for morphological changes, transduction efficiency and osteoblast differentiation.

3D: hMSCs grown until 90% confluent were transduced with AdBMP9 + Polybrene 8μg/ml diluted in DMEM at MOI 100. Following 4 h of incubation at 37°C and 5% CO2, 3×10^5 cells were washed, trypsinized, and seeded onto 8 mm discs of mineralized collagen-glycosaminoglycans (MC-GAG) scaffolds. 24 hours after seeding, cells were subjected to differentiation medium as described above

ELISA

Culture supernatants were collected from control and AdBMP-9 transduced primary hMSCs and concentrated from 1 mL to 100 μL. BMP-9 protein concentrations were determined using the human BMP9 DuoSet ELISA kit (R&D Systems, Minneapolis, MN) according to manufacturer's instructions. Briefly, a 96-well microplate was coated with the capture antibody and incubated overnight at room temperature. After blocking, samples were incubated for 2 hours at room temperature with the detection antibody, washed, and incubated with streptavidin-HRP for 20 min. 20 min after addition of the substrate solution, the reaction was stopped by adding 100 μL of 2N H_2SO_4. Plates were read at 450 and 570 nm wavelengths on the Epoch microplate reader (BioTex, Winooski, VT).

Alkaline phosphatase histochemical staining

An alkaline phosphatase (ALP) histochemical diagnostic kit (Sigma, St. Louis, MO) was used to detect the expression of ALP as a sign of early osteoblast differentiation using manufacturer's instructions. Briefly, cells were fixed with citrate-acetone-formaldehyde fixative solution for 1 minute at room temperature, washed, and incubated with a mixture of naphthol AS-BI and diazonium salt solution at room temperature for 30 min. Cells were then rinsed in deionized water and evaluated microscopically.

Flow Cytometry

7 days after transduction of hMSCs with adenoviruses, the medium was removed. The cells were washed twice with PBS. Cells were detached with Accutase (Innovative Cell Technologies, San Diego, CA) and centrifuged at 400 g for 5 mins. After washing, cell pellets were resuspended in FACS buffer. The percentage of cells expressing GFP was then measured using FACS Jazz (BD Biosciences, Franklin Lakes, NJ).

Quantitative real-time reverse-transcriptase polymerase chain reaction

Scaffolds were processed for total RNA extraction using the RNeasy kit (Qiagen, Valencia, CA) at 0, 3, and 14 days. Quantitative real-time reverse-transcriptase polymerase chain reaction (RT-PCR) was performed on the Opticon Continuous Fluorescence System (Bio-Rad Laboratories, Inc., Hercules, CA) using the QuantiTect SYBR Green RT-PCR kit (Qiagen, Valencia, CA). Cycle conditions were as follows: reverse transcription at 50°C (30 minutes); activation of HotStarTaq DNA polymerase/inactivation of reverse transcriptase at 95°C (15 minutes); and 45 cycles of 94°C for 15 seconds, 58°C for 30 seconds, and 72°C for 45 seconds. Results were analyzed using the comparative CT method for analyzing reverse-transcriptase polymerase chain reaction data and presented as representative graphs of triplicate experiments. Primer sequences are listed in Table 1.

Western blot

Lysates for western blot analysis were prepared from scaffolds at 0, 3, 7, 14, and 21 days of culture using Phosphosafe lysis buffer (Novagen, Madison, WI). Equal amounts of protein lysates were subjected to 4–20% SDS-PAGE (Bio-Rad, Hercules, CA). Western analysis was carried out with antibodies against phosphorylated-Smad1/5 (p-Smad1/5), total Smad1/5/8, phosphorylated-ERK1/2 (p-ERK1/2), total ERK1/2, phosphorylated-Smad2/3

(p-Smad2/3), total Smad2/3, phosphorylated-p38 (p-p38), total p38, and β-actin followed by 1:4000 dilutions of horseradish peroxidase-conjugated IgG antibodies (Bio-Rad, Hercules, CA) and an enhanced chemiluminescent substrate (Thermo Scientific, Rockford, IL). All primary phospho and full length antibodies were obtained from Cell Signaling Technologies (Beverly, MA) except Smad1/5/8, which was obtained from Santa Cruz Biotechnology (Santa Cruz, CA). Imaging was carried out using ImageJ (NIH, Bethesda, MD).

Histology and immunohistochemistry

Histologic studies were performed on scaffold cultures at 7 days, 14 days, and 6 weeks. Scaffolds were fixed at 10% normal buffered formalin, embedded in paraffin, and sectioned at 4 microns using standard techniques. The sections were deparaffinized and stained with hematoxylin and eosin, Alizarin Red, or Alcian Blue and van Gieson (American Mastertech Scientific, Lodi, CA) and processed with the Dako automated FLEX system (Dako, Carpinteria, CA). All slides were analyzed qualitatively using a standard microscope and digitally photographed.

Micro–Computed Tomographic Imaging

Mineralization was followed by micro–computed tomographic imaging (μCT) using the Scanco μCT 35 (Scanco Medical AG, Bruttisellen, Switzerland) at 6 and 12 weeks in culture ($n = 3$ scaffolds per time point). Scaffolds were fixed using 10% formalin for 24 hours and stored in 70% ethanol at 4°C. Scans were performed using medium resolution settings with a source voltage of 70 E (kVp) and I (μA) of 114. The images had a final element size of 12.5 μm. Two-dimensional images were analyzed using software supplied from Scanco (Image Processing Language version 5.6). Scaffold areas were contoured to establish volumes of interest by visual examination of serial slices in all of the specimens. Optimum arbitrary threshold values of 20 (showing scaffold and mineralization) and 80 (mineralization alone) were used uniformly for all specimens to quantify mineralized areas from surrounding unmineralized scaffold. Histomorphometric analysis of three-dimensional reconstructions was performed using Scanco Evaluation scripts no. 2 (three-dimensional segmentation of two volumes of interest: solid dense in transparent low-density object) for three-dimensional images and script no. 6 (bone volume/density only bone evaluation) for volume determinations.

Statistical Analysis

All analysis was performed using SPSS software (SPSS, Inc., Chicago, IL). Two-tailed paired sample *t* tests were performed to evaluate the BMP-9 protein and gene expression (Figure 1) and ALP activity (Figure 2). Analysis of variance was used to evaluate the effect of BMP-9 transduction and time on osteogenic gene expression, chondrogenic gene expression, and mineralization (Figures 3, 4, 6). The F statistic, associated degrees of freedom, and p values are reported. For post hoc comparisons between groups using the Tukey criterion, p values are reported. A value of $p<0.05$ was considered significant.

Results

BMP-9 induces osteogenic differentiation in primary hMSCs in two-dimensional cultures

Although multiple investigators have demonstrated osteogenic abilities of BMP-9, cell type and origin differences may influence responses to growth factors. To confirm that our primary bone marrow derived human mesenchymal stem cells (hMSCs) responded similarly to published work, control and AdBMP-9 transduced hMSCs were cultured in osteogenic differentiation medium for 7 days and evaluated for infection efficiency and BMP-9 expression (Figure 1). Using the co-expressed GFP as an indicator, AdBMP-9 transduction resulted in a 35% infection efficiency based on flow cytometry of fluorescent cells in comparison to non-infected cells (Figure 1A). Transcription of BMP-9 was verified using quantitative RT-PCR and found to be significantly higher than control cells at day 7 (Figure 1B). To verify BMP-9 protein expression and secretion, culture supernatants of hMSCs transduced with BMP-9 or control were harvested at day 7 and subjected to ELISA (Figure 1C). While BMP-9 protein was undetectable in control supernatants, BMP-9 approached 600 pg/mL in transduced supernatants.

The effect of BMP-9 on osteogenic differentiation was evaluated using alkaline phosphatase (ALP) activity assays and histologic mineralization (Figure 2). At 7 and 14 days after transduction, control and BMP-9 transduced primary hMSCs cultured in osteogenic medium demonstrated ALP activity. However, at both timepoints, BMP-9 increased the number of cells expressing ALP and the intensity of staining. Both qualitatively and quantitatively (Figure 2A and B, respectively), ALP activity was higher in BMP-9 expressing cultures. Similarly, mineralization of hMSCs was also evaluated using Alizarin red staining at 14 and 21 days in culture with osteogenic medium (Figure 2C). At day 14 of culture, some mineralization was detected in control cultures, as expected [21]. Mineralized content in control cultures increased from day 14 to 21. In contrast, BMP-9 treated cultures demonstrated a far greater amount of Alizarin red staining at both time points. This confirmed that BMP-9 strongly induced osteogenic differentiation in two dimensional cultures of primary human mesenchymal stem cells.

BMP-9 induces differences in ALP gene expression but not differences in other osteogenic genes or mineralization in hMSCs on MC-GAG scaffold

With the confirmation that BMP-9 induces osteogenesis in hMSCs in two-dimensional cultures in our system, we evaluated lineage commitment in three-dimensions on MC-GAG scaffolds. Control and AdBMP-9 transduced hMSCs were cultured in osteogenic differentiation medium on MC-GAG scaffolds and subjected to quantitative RT-PCR for alkaline phosphatase (ALP), type I collagen (Col I), and osteopontin (OPN) expression (Figure 3A–C). An analysis of variance (ANOVA) comparing BMP-9 transduction on gene expression over time revealed a significant difference on ALP [$F(5,12)=18.350$, $p<0.001$] and OPN [$F(5,12)=19.020$, $p<0.001$]. As we previously reported [15], MC-GAG scaffolds induced an increase in ALP, Col I, and OPN expression in hMSCs when cultured in osteogenic medium when normalized to day 0 values. The addition of BMP-9 induction led to an increase in ALP expression on day 14 when compared to untreated scaffold ($p<0.01$) as well as in comparison to day 3 expression levels ($p<0.001$). In Col I expression, a multi-

fold increase in expression relative to day 0 levels was present at every timepoint. However, no statistically significant differences were found between hMSCs cultured on MC-GAG or MC-GAG/BMP-9 or over time. Similar to Col I, OPN expression also demonstrated a multi-fold increase in expression relative to day 0 levels. OPN expression did not vary significantly between untreated and BMP-9 treated scaffolds. However, in both untreated and BMP-9 treated groups, OPN expression decreased over time ($p<0.001$ and $p<0.01$, respectively). Thus, BMP-9 treatment of primary hMSCs on MC-GAG scaffolds demonstrated differences in ALP expression but no significant differences in Col I and OPN expression.

To confirm that transduction of BMP-9 occurred successfully in three dimensional cultures, both gene expression and protein secretion were evaluated (Figure 3D–E). ANOVA comparisons demonstrated significant effects for both BMP-9 gene expression [$F(5,12)=40.836$, $p<0.001$] and protein secretion [$F(10,22)=66.031$, $p<0.001$]. Similar to the two-dimensional cultures, expression of BMP-9 was minimal at all timepoints in control cells, whereas BMP-9 transduced cells demonstrated large elevations of transcripts on MC-GAG scaffolds (Figure 3D). Secretion of BMP-9 protein was compared in control and BMP-9 transduced cells (Figure 3E). Paralleling the quantitative PCR data, secreted BMP-9 was found in significantly greater quantities in BMP-9 transduced cells in comparison to control cells. For both mRNA and protein expression, BMP-9 appeared to be produced in the greatest quantities at day 3, followed by a steep decrease in transcripts and secreted protein ($p<0.001$) although elevated levels continued to be detected even after 6 weeks of culture.

BMP-9 increases expression of markers of chondrogenesis and cartilage staining in hMSCs on MC-GAG scaffolds

To determine the contribution of BMP-9 to mineralization of hMSCs on MC-GAG scaffolds, quantification of mineralized content was evaluated with micro-CT scanning and subjected to ANOVA for statistical analysis (Figure 4). There was a significant effect of time and treatment on the quantity of mineralized content found on the scaffolds [$F(5,12)=8.726$, $p=0.001$]. Similar to our previous reports [15, 22], MC-GAG induced hMSC mineralization in the absence of any growth factors both qualitatively and quantitatively at 4, 6, and 8 weeks of culture. Between 4 and 8 weeks, both untreated and BMP-9 treated scaffolds demonstrated increases in mineralization at the later timepoints when compared to earlier timepoints ($p<0.05$ and $p<0.01$, respectively). However, no statistically significant differences in mineralization occurred at any of the timepoints between the untreated and treated groups. Thus, no significant increase in hMSC mineralization occurred on MC-GAG scaffolds in the absence of presence of BMP-9.

Interestingly, histologic analyses of scaffolds demonstrated differences in extracellular matrix deposition (Figure 5). Cellular infiltration was found throughout the entirety of the scaffold and was equivalent in the absence or presence of BMP-9. Similar to the micro-CT data, mineralization was detected in all scaffolds via Alizarin red staining from day 7 to 6 weeks with no appreciable differences between control and BMP-9 treated cells. However, when sections were stained with Alcian blue to detect sulfated glycosaminoglycans, hMSCs

transduced with BMP-9 demonstrated increased staining at all timepoints with intensification at 6 weeks of culture, suggestive of differentiation into cartilage.

To correlate the histologic staining with gene expression, four chondrogenic markers were evaluated in quantitative RT-PCR on hMSCs cultured on MC-GAG in the absence and presence of BMP-9 (Figure 6A–D). The results were subjected to ANOVA which revealed significant gene expression differences in Sox9 [$F(5,12)=21.774$, $p<0.001$], Col2a1 [$F(5,12)=16.191$, $p<0.001$], ACAN [$F(5,12)=6.832$, $p=0.003$], and COMP [$F(5,12)=5.087$, $p=0.01$]. Gene expression of both Sox9 transcription factor and type II collagen (Col2a1) were significantly induced at day 14 only in BMP-9 treated cells when compared to untreated cells ($p<0.001$). Both Sox9 and Col2a1 gene expression at day 14 were significantly increased in comparison to day 3 ($p<0.001$). Aggrecan (ACAN) and cartilage oligomeric matrix protein (COMP), both of which are cartilage-related extracellular matrix genes, were also significantly induced only in BMP-9 treated cells, albeit at an earlier timepoint (day 7). To evaluate whether these increases in expression were secondary to the formation of hypertrophic chondrocytes in the process of endochondral ossification [23], collagen X (Col10A1) was evaluated (Figure 6E). Unlike all of the former four chondrogenic markers, no statistically significant differences could be detected in Col10A1 expression. Taken together, BMP-9 induces chondrocyte differentiation and increased production of sulfated glycosaminoglycans in hMSCs on MC-GAG scaffolds with no histologic or quantitative differences in mineralization or increases in expression of a hypertrophic chondrocyte marker.

BMP-9 activates the non-canonical BMPR signaling pathway in hMSCs cultured on MC-GAG scaffolds

We have previously demonstrated that MC-GAG constitutively induces activation of the canonical BMPR signaling pathway via Smad1/5 phosphorylation in hMSCs [15]. To elucidate the signaling mechanisms induced by BMP-9 in hMSCs on MC-GAG scaffolds, the Smad dependent and independent pathways of BMP receptor signalling were investigated (Figure 7). Western blot analyses demonstrated that p-Smad1/5 was constitutively phosphorylated in control and BMP-9 cells at all timepoints during culture. Thus, addition of BMP-9 did not appreciably change Smad-dependent BMP receptor signalling activated by MC-GAG.

To evaluate the non-canonical BMP receptor pathways, p-ERK1/2, p-Akt, p-p38, p-Smad2/3, and p-JNK were compared to the respective total protein. In the absence of BMP-9, p-ERK1/2 was minimally detected until day 14 and remained elevated thereafter. Both p-Akt and p-p38 were undetectable until day 7 in untreated cells. While p-Akt decreased at later timepoints, p-p38 remained present through the latest timepoint (day 21). In contrast, both p-ERK1/2 and p-p38 demonstrated increased expression in the presence of BMP-9 throughout all timepoints. With BMP-9, both p-ERK1/2 and p-p38 were detectable earlier by day 3. P-Akt demonstrated detectable protein expression by day 3 with expression peaking at day 7, following by minimal expression thereafter. Mild to no differences in Smad2/3 or JNK phosphorylation were found in the absence or presence of BMP-9. Thus,

the addition of BMP-9 activated the non-canonical, Smad-independent BMP receptor signaling pathways, specifically ERK1/2, Akt, and p38 MAPK.

Discussion

In this work, we investigated the contribution of BMP-9 stimulation to differentiation of hMSCs on mineralized collagen glycosaminoglycan scaffolds. In two-dimensional cultures, BMP-9 induced osteogenic differentiation and mineralization similar to reports in the literature. On three-dimensional MC-GAG scaffolds, hMSCs treated with BMP-9 did not result in significant increases in osteogenic gene expression or mineralization radiographically or histologically. Instead, BMP-9 induced production of sulfated glycosaminoglycans seen in cartilage-specific matrix that increased with time, correlating to upregulation of cartilage specific-extracellular matrix genes. Of note, collagen X, a marker of chondrocyte hypertrophy was not induced by BMP-9 in hMSCs on MC-GAG scaffolds. Addition of BMP-9 did not increase Smad1/5 activation in hMSCs on MC-GAG scaffolds. However, ERK1/2, p38, and Akt, intracellular members of the non-canonical BMPR signaling pathway, were activated earlier and in greater amounts than in hMSCs cultured on MC-GAG without BMP-9. Taken together, our data suggests that hMSCs treated with BMP-9 on nanoparticulate mineralized collagen glycosaminoglycan scaffolds differentiate into a stable composite of mineralized and cartilaginous content.

The reasons for evaluating BMP-9 on MC-GAG-mediated hMSC osteogenic differentiation were threefold. We have previously reported that the MC-GAG scaffold is a highly osteogenic material for primary bone marrow-derived mesenchymal stem cells characterized with a porosity of 85 ± 3 % [24], pore size of 156 ± 6 μm [19, 24], and morphology of isotropic pores with a transverse:longitudinal pore aspect ratio of 0.95 ± 0.01 [19]. In comparison to non-mineralized collagen glycosaminoglycan scaffolds, MC-GAG has an increased stiffness and the ability to release calcium and phosphate ions from the scaffold into culture, which may be contributors to the osteogenic capabilities [17, 25]. Although we have shown that MC-GAG induces osteogenesis efficiently in the absence of BMP-2 [15, 22], BMP-9 has been demonstrated to be the most osteogenic BMP family member in both *in vitro* and *in vivo* ectopic mineralization studies using C3H10T1/2 cells and C2C12 cells [3, 26]. Thus, a comparison between scaffold-mediated and scaffold/growth factor-mediated osteogenesis was important to understand whether additional modifications of the scaffold could be performed. Secondly, while BMP-9 has been associated to activation of endochondral ossification, the MC-GAG scaffold has only demonstrated intramembranous ossification of hMSCs. Thus, we sought to gain an understanding of whether additive effects of endochondral and intramembranous ossification would occur. Lastly, BMP-2 and MC-GAG both stimulate hMSC differentiation primarily via the canonical, Smad1/5 dependent BMPR signaling pathway [15, 22]. However, several investigators have demonstrated differences in BMP-9 signalling including receptor affinity [27]. Thus, we also sought to understand whether stimulating alternative BMP receptor signaling pathways would contribute to increased mineralization. Based on the data from our current work, hMSC mineralization mediated by MC-GAG scaffolds did not increase in the presence of BMP-9. In combination with our previous work that demonstrated mineralization independent from BMP-2 [15, 22], our current work provides additional evidence that MC-GAG is a viable

material-based strategy for bone regeneration that does not require exogenous growth factor addition. In addition, BMP receptor signaling via BMP-9 stimulation generated activation of both cartilage-specific gene expression as well as deposition of sulfated glycosaminoglycans in long term cultures. In combination, these data suggest a potential for harnessing the differential properties of MC-GAG and BMP-9 in generation of a bone cartilage construct.

Differences exist in intracellular signaling pathways induced by BMP-9 in two-dimensional cultures versus three-dimensional MC-GAG scaffolds. In this work, we did not explicitly examine the two-dimensional signaling mechanisms for BMP-9 mediated osteogenic differentiation, however, this has been well reported in the literature. Using C3H10T1/2 mesenchymal progenitor cells and C2C12 osteoblast progenitor cells in two-dimensional cultures, Luo and colleagues demonstrated that BMP-9 induced osteogenic differentiation via activation of Smad1/5/8, p38, and ERK1/2 [7, 28]. While both Smad1/5/8 and p38 inhibition disrupted osteogenic differentiation, ERK1/2 inhibition increased osteogenic differentiation. Subsequently, their group also demonstrated that JNKs were activated in response to BMP-9 in C3H10T1/2, C2C12, and primary bone marrow stromal cells [8]. JNK inhibition prevented Smad1/5/8 activation and decreased mineralization. In primary periodontal ligament stem cells (PDLSCs), Ye and colleagues similarly showed that BMP-9 induces osteogenic differentiation with activation of osteogenic gene expression and mineralization [6]. Similar to C3H10T1/2 and C2C12 cells, p38 inhibition decreased whereas ERK1/2 inhibition increased osteogenic differentiation of PDLSCs. In a study to delineate the contributions of insulin growth factor-2 (IGF-2) to BMP-9 mediated osteogenic differentiation in C3H10T1/2 cells, Chen and colleagues showed that BMP-9 activates Smad1/5/8 phosphorylation but has no effect on the PI3K/Akt pathway [29]. Similar to two-dimensional scaffolds, our Western blot results (Figure 7) demonstrated that BMP-9 treatment correlated to p38 and ERK1/2 activation. Unlike two-dimensional cultures, Akt phosphorylation was increased in response to BMP-9 treatment. JNK phosphorylation, unlike two-dimensional cultures, was not induced in response to BMP-9 treatment. Furthermore, phosphorylation of Smad1/5 was elevated on three-dimensional scaffolds regardless of BMP-9 activation. Although our current study is limited in the understanding of differential intracellular signaling pathway activation, clear differences exist between osteogenic differentiation of mesenchymal stem cells in response to BMP-9 between two-dimensional cultures and MC-GAG scaffolds. Such differences suggest potential targets for further directing hMSC differentiation bone and cartilage composites.

Several investigators have evaluated the utility of BMP-9 and other BMPs in scaffold-based regenerative strategies and found significant differences in osteogenesis with different scaffold compositions. He and colleagues characterized *in* vivo osteogenic differentiation of C2C12 cells on type I collagen, hydroxyapatite tricalcium phosphate (HA-TCP), and demineralized bone matrix (DBM) scaffold carriers [26]. These studies demonstrated that ectopic bone formation occurred in greater quantities in collagen and HA-TCP scaffolds in comparison to DBM. Using a truncated, osteogenic BMP-9 peptide, Faucheux and colleagues demonstated *in vivo* osteogenesis of MC3T3 cells as ectopic bone with chitosan but not collagen scaffolds [30]. The combination of these investigations and our current study highlight the instructive abilities for scaffold composition and suggests potential for developing microenvironments with differential scaffold elements.

Transient versus permanent chondrocytic differentiation continues to be a central obstacle in any investigation for cartilage regeneration. The question of whether BMP-9 is inducing stable cartilage versus endochondral ossification must be asked. In our system, there are three pieces of evidence that suggest chondrocyte stability. First, addition of BMP-9 resulted in an increase in sulfated glycosaminoglycans that increased with time. Second, BMP-9 did not increase collagen X expression, typically found in hypertrophic chondrocytes, suggesting that these cells are not currently undergoing endochondral ossification. Third, BMP-9 treatment increased both Sox9 and collagen II expression, coincident with a decrease in osteopontin expression. Sox9 expression, in particular, is significant in that other investigators have recently shown that Sox9 overexpression both potentiates chondrocytic differentiation as well as inhibits BMP-2 mediated osteogenic differentiation [31]. Our data suggests that, in the setting of MC-GAG, BMP-9 increases chondrocytic differentiation of hMSCs via activation of the non-canonical BMP receptor signaling pathway and upregulation of Sox9.

One of the defining characteristics of the osteochondral junction is the zonal architecture with gradual transition from mature cartilage to chondrocytes intermixed within mineralized bone and, finally, to mature subchondral bone. The opposing instructive effects of MC-GAG and BMP-9 may be potentially harnessed to generate a biphasic construct consisting of cartilage and mineralized bone. Our current report suggests a potential construct that warrants future *in vivo* testing.

Acknowledgments

This work was supported by the US Department of Veterans Affairs under award numbers IK2 BX002442-01A2 (JCL) and 1I01BX001367-01A2 (TAM), the Jean Perkins Foundation (JCL), the Aramont Foundation (TAM), and the Bernard G. Sarnat Endowment for Craniofacial Biology (JCL). Research reported in this publication was also supported by the National Institute of Arthritis and Musculoskeletal and Skin Diseases of the National Institutes of Health under award number R21 AR063331 (BACH). The content is solely the responsibility of the authors and does not necessarily represent the official views of the National Institutes of Health. DWW was funded at UIUC from National Science Foundation (NSF) Grant 0965918 IGERT: Training the Next Generation of Researchers in Cellular & Molecular Mechanics and BioNanotechnology.

References

1. Gadjanski I, Vunjak-Novakovic G. Expert Opin Biol Ther. 2015; 15:1583. [PubMed: 26195329]
2. Ducy P, Karsenty G. Kidney Int. 2000; 57:2207. [PubMed: 10844590] Mueller TD, Nickel J. FEBS Lett. 2012; 586:1846. [PubMed: 22710174]
3. Cheng H, Jiang W, Phillips FM, Haydon RC, Peng Y, Zhou L, Luu HH, An N, Breyer B, Vanichakarn P, Szatkowski JP, Park JY, He TC. J Bone Joint Surg Am. 2003; 85-A:1544. [PubMed: 12925636]
4. Kang Q, Sun MH, Cheng H, Peng Y, Montag AG, Deyrup AT, Jiang W, Luu HH, Luo J, Szatkowski JP, Vanichakarn P, Park JY, Li Y, Haydon RC, He TC. Gene Ther. 2004; 11:1312. [PubMed: 15269709] Kang Q, Song WX, Luo Q, Tang N, Luo J, Luo X, Chen J, Bi Y, He BC, Park JK, Jiang W, Tang Y, Huang J, Su Y, Zhu GH, He Y, Yin H, Hu Z, Wang Y, Chen L, Zuo GW, Pan X, Shen J, Vokes T, Reid RR, Haydon RC, Luu HH, He TC. Stem Cells Dev. 2009; 18:545. [PubMed: 18616389] Nakamura T, Shinohara Y, Momozaki S, Yoshimoto T, Noguchi K. Biochem Biophys Res Commun. 2013; 440:289. [PubMed: 24064349]
5. Li C, Yang X, He Y, Ye G, Li X, Zhang X, Zhou L, Deng F. Int J Med Sci. 2012; 9:862. [PubMed: 23155360]

6. Ye G, Li C, Xiang X, Chen C, Zhang R, Yang X, Yu X, Wang J, Wang L, Shi Q, Weng Y. Int J Med Sci. 2014; 11:1065. [PubMed: 25136261]
7. Zhao Y, Song T, Wang W, Wang J, He J, Wu N, Tang M, He B, Luo J. PLoS One. 2012; 7:e43383. [PubMed: 22912865]
8. Zhao YF, Xu J, Wang WJ, Wang J, He JW, Li L, Dong Q, Xiao Y, Duan XL, Yang X, Liang YW, Song T, Tang M, Zhao D, Luo JY. BMB Rep. 2013; 46:422. [PubMed: 23977991]
9. Lopez-Coviella I, Mellott TM, Kovacheva VP, Berse B, Slack BE, Zemelko V, Schnitzler A, Blusztajn JK. Brain Res. 2006; 1088:49. [PubMed: 16626664]
10. Lam J, Lu S, Kasper FK, Mikos AG. Adv Drug Deliv Rev. 2015; 84:123. [PubMed: 24993610]
11. Majumdar MK, Wang E, Morris EA. J Cell Physiol. 2001; 189:275. [PubMed: 11748585]
12. Blunk T, Sieminski AL, Appel B, Croft C, Courter DL, Chieh JJ, Goepferich A, Khurana JS, Gooch KJ. Growth Factors. 2003; 21:71. [PubMed: 14626354]
13. Neumann AJ, Alini M, Archer CW, Stoddart MJ. Tissue Eng Part A. 2013; 19:1285. [PubMed: 23289669] Sailor LZ, Hewick RM, Morris EA. J Orthop Res. 1996; 14:937. [PubMed: 8982137]
14. Lee JC, Pereira CT, Ren X, Huang W, Bischoff D, Weisgerber DW, Yamaguchi DT, Harley BA, Miller TA. J Craniofac Surg. 2015
15. Ren X, Bischoff D, Weisgerber DW, Lewis MS, Tu V, Yamaguchi DT, Miller TA, Harley BA, Lee JC. Biomaterials. 2015; 50:107. [PubMed: 25736501]
16. Harley BA, Leung JH, Silva EC, Gibson LJ. Acta Biomater. 2007; 3:463. [PubMed: 17349829] Harley BA, Lynn AK, Wissner-Gross Z, Bonfield W, Yannas IV, Gibson LJ. J Biomed Mater Res A. 2010; 92:1066. [PubMed: 19301274]
17. Weisgerber DW, Kelkhoff DO, Caliari SR, Harley BA. J Mech Behav Biomed Mater. 2013; 28:26. [PubMed: 23973610]
18. Olde Damink LH, Dijkstra PJ, van Luyn MJ, van Wachem PB, Nieuwenhuis P, Feijen J. Biomaterials. 1996; 17:765. [PubMed: 8730960]
19. Weisgerber DW, Kelkhoff DO, Caliari SR, Harley BAC. J Mech Behav Biomed Mater. 2013; 28:26. [PubMed: 23973610]
20. Caliari SR, Gonnerman EA, Grier WK, Weisgerber DW, Banks JM, Alsop AJ, Lee J-S, Bailey RC, Harley BAC. Advanced healthcare materials. 2014; 3:1086. [PubMed: 24574180]
21. Huang W, Carlsen B, Wulur I, Rudkin G, Ishida K, Wu B, Yamaguchi DT, Miller TA. Exp Cell Res. 2004; 299:325. [PubMed: 15350532]
22. Ren X, Tu V, Bischoff D, Weisgerber DW, Lewis MS, Yamaguchi DT, Miller TA, Harley BA, Lee JC. Biomaterials. 2016; 89:67. [PubMed: 26950166]
23. Apte SS, Seldin MF, Hayashi M, Olsen BR. Eur J Biochem. 1992; 206:217. [PubMed: 1587271]
24. Harley BA, Lynn AK, Wissner-Gross Z, Bonfield W, Yannas IV, Gibson LJ. J Biomed Mater Res A. 2010; 92:1066. [PubMed: 19301274]
25. Weisgerber DW, Caliari SR, Harley BA. Biomater Sci. 2015; 3:533. [PubMed: 25937924]
26. Shui W, Zhang W, Yin L, Nan G, Liao Z, Zhang H, Wang N, Wu N, Chen X, Wen S, He Y, Deng F, Zhang J, Luu HH, Shi LL, Hu Z, Haydon RC, Mok JM, He TC. J Biomed Mater Res A. 2014; 102:3429. [PubMed: 24133046]
27. Luo J, Tang M, Huang J, He BC, Gao JL, Chen L, Zuo GW, Zhang W, Luo Q, Shi Q, Zhang BQ, Bi Y, Luo X, Jiang W, Su Y, Shen J, Kim SH, Huang E, Gao Y, Zhou JZ, Yang K, Luu HH, Pan X, Haydon RC, Deng ZL, He TC. J Biol Chem. 2010; 285:29588. [PubMed: 20628059]
28. Xu DJ, Zhao YZ, Wang J, He JW, Weng YG, Luo JY. BMB Rep. 2012; 45:247. [PubMed: 22531136]
29. Chen L, Jiang W, Huang J, He BC, Zuo GW, Zhang W, Luo Q, Shi Q, Zhang BQ, Wagner ER, Luo J, Tang M, Wietholt C, Luo X, Bi Y, Su Y, Liu B, Kim SH, He CJ, Hu Y, Shen J, Rastegar F, Huang E, Gao Y, Gao JL, Zhou JZ, Reid RR, Luu HH, Haydon RC, He TC, Deng ZL. J Bone Miner Res. 2010; 25:2447. [PubMed: 20499340]
30. Bergeron E, Leblanc E, Drevelle O, Giguère R, Beauvais S, Grenier G, Faucheux N. Tissue Eng Part A. 2012; 18:342. [PubMed: 21902464]
31. Liao J, Hu N, Zhou N, Lin L, Zhao C, Yi S, Fan T, Bao W, Liang X, Chen H, Xu W, Chen C, Cheng Q, Zeng Y, Si W, Yang Z, Huang W. PLoS One. 2014; 9:e89025. [PubMed: 24551211]

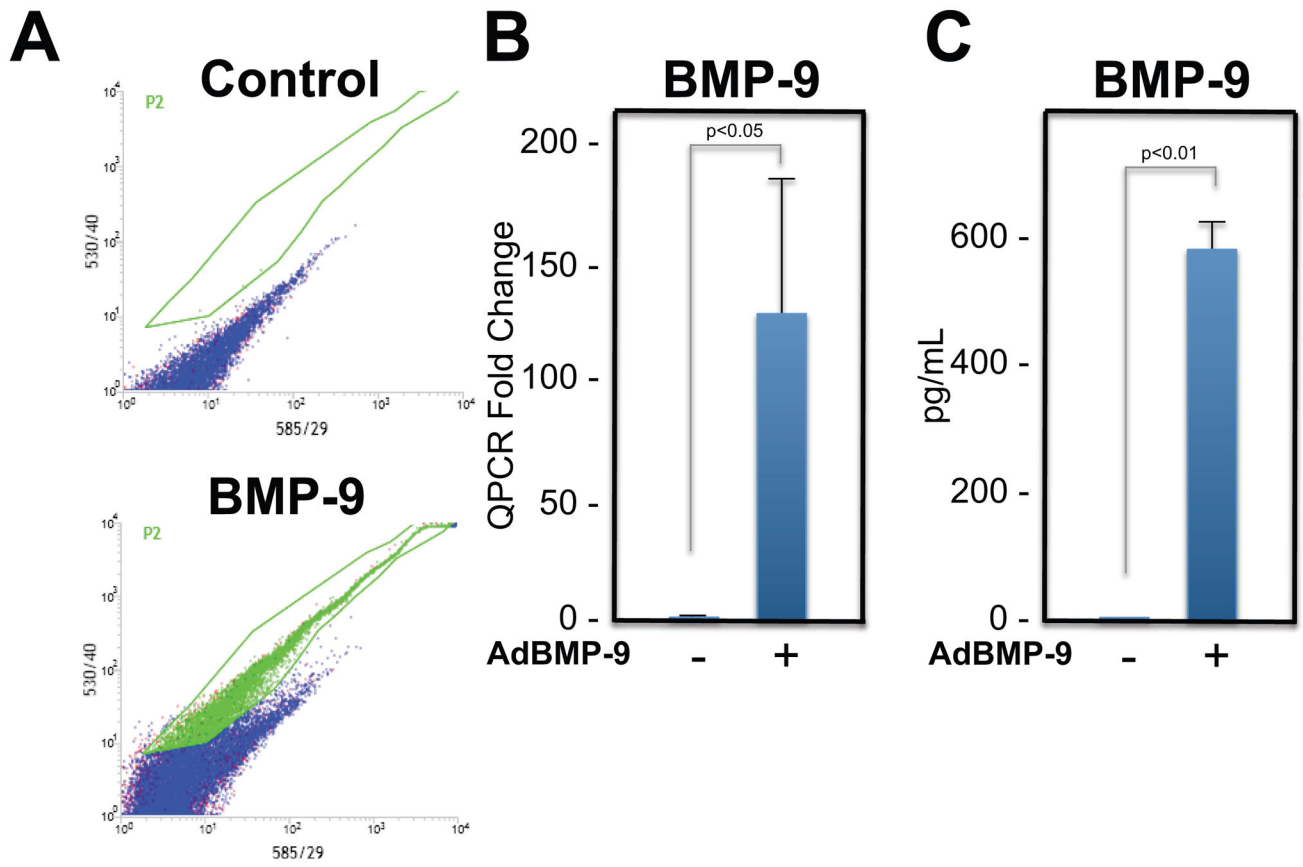

Figure 1. AdBMP-9 transduction in hMSCs induces BMP-9 expression and secretion in two dimensional cultures

A) FACS analysis of GFP expression in AdBMP-9 infected hMSCs in comparison to control. B) Quantitative RT-PCR of BMP-9 in hMSCs 7 days after AdBMP-9 infection (normalized to day 0). C) ELISA for BMP-9 secretion in culture media 7 days after infection.

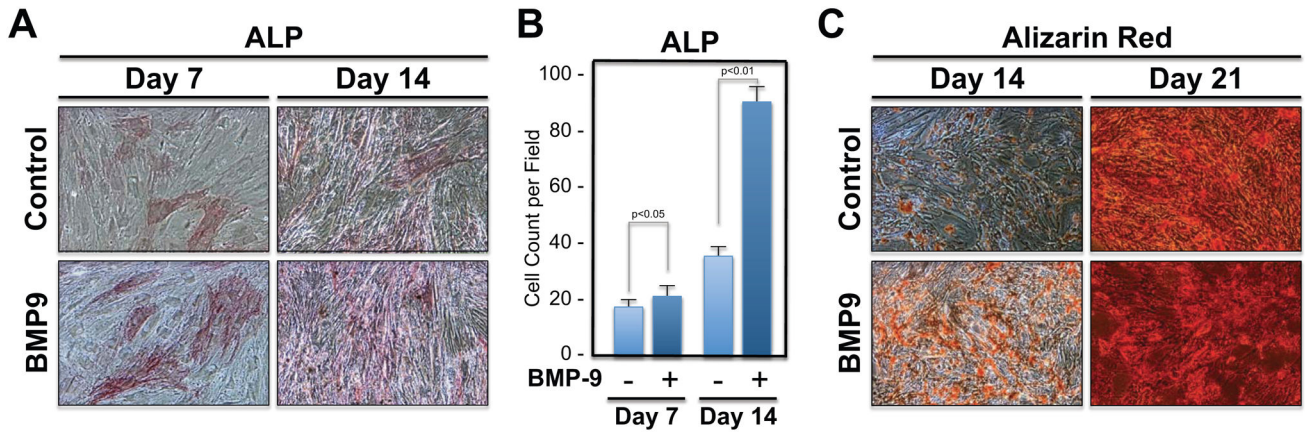

Figure 2. Alkaline phosphatase activity and mineralization of hMSCs transduced with AdBMP-9 in two dimensional cultures

A) ALP expression in control and BMP-9 expressing hMSCs on days 7 and 14. B) Quantitative analysis of ALP expressing cells on days 7 and 14. C) Alizarin red staining in control and BMP-9 expressing hMSCs on days 14 and 21.

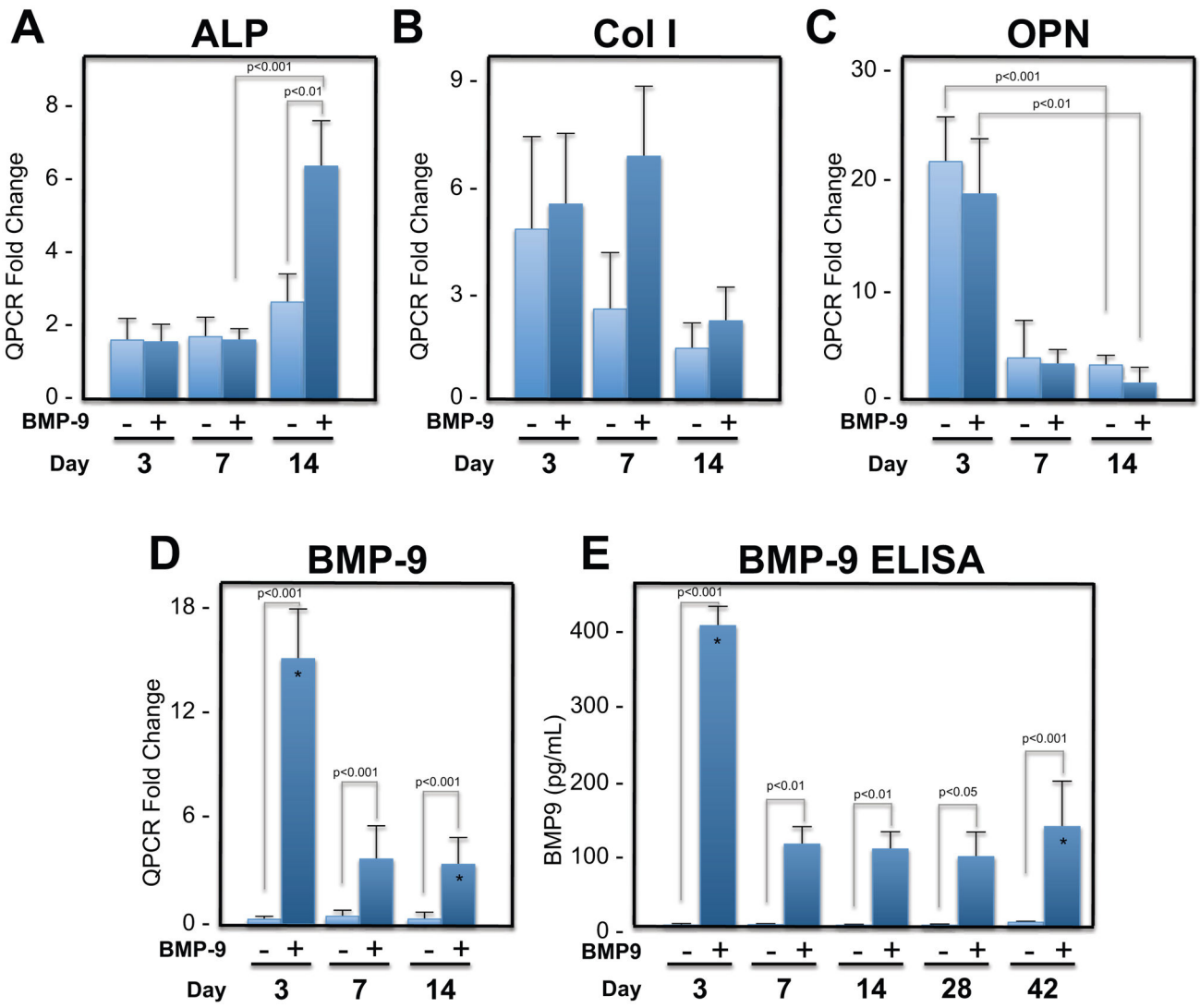

Figure 3. Expression of osteogenic genes and BMP-9 following AdBMP-9 infection in hMSCs on MC-GAG scaffolds

Quantitative RT-PCR normalized to day 0 of A) alkaline phosphatase (ALP), B) type I collagen (Col I), C) osteopontin (OPN), and D) BMP-9 in hMSCs on MC-GAG at 3, 7, and 14 days in the absence and presence of AdBMP-9 transduction. E) Concentration of BMP-9 secretion in culture supernatants quantified by ELISA. P values are indicated as shown. In addition, * denotes $p<0.001$ between indicated timepoints.

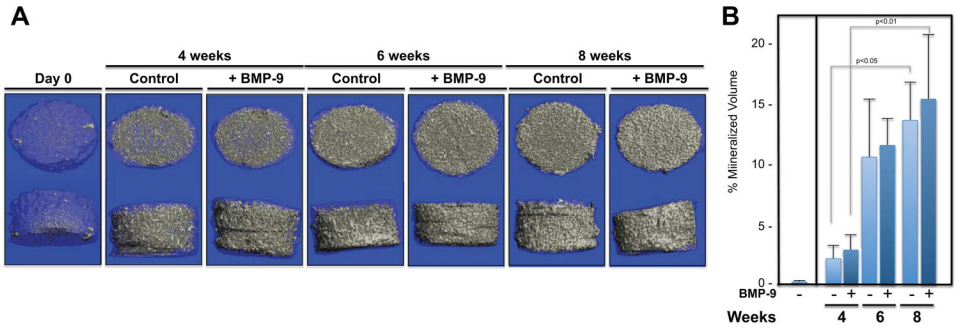

Figure 4. micro-CT scans of hMSCs cultured on MC-GAG scaffolds in the absence and presence of BMP-9

A) Representative 3D reconstructed μCT scans of collagen scaffolds cultured with hMSCs in osteogenic medium in the presence or absence of BMP-9 for 4, 6, and 8 weeks on MC-GAG scaffolds. B) Quantification of mineralized content on μCT scans in triplicate.

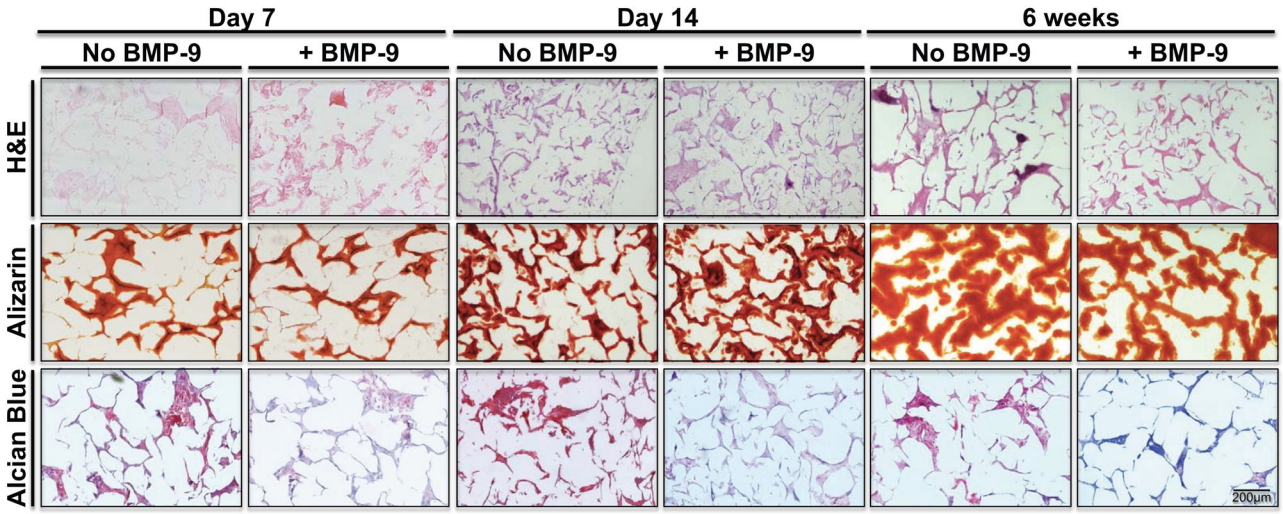

Figure 5. Histology of hMSCs undergoing osteogenesis on MC-GAG scaffolds in the absence and presence of BMP-9

H&E (top panels), Alizarin Red (middle panels), and Alcian Blue/van Giesen (bottom panels) staining of histologic sections of Col-GAG and MC-GAG scaffolds cultured with hMSCs in osteogenic medium in the presence or absence of BMP-9 at 7 days, 14 days, and 6 weeks. (Magnification, 10X; scale bar, 200 μm)

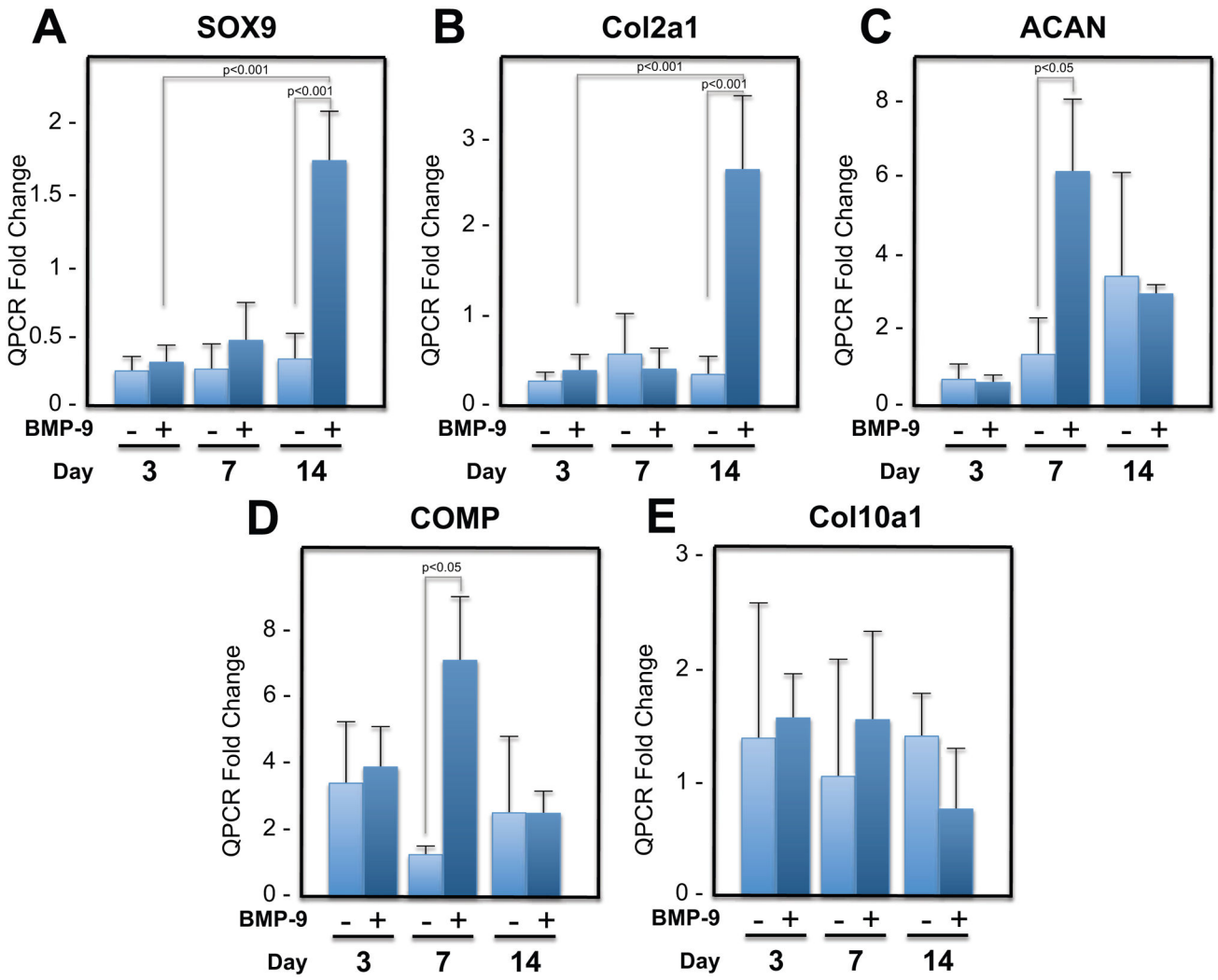

Figure 6. Expression of chondrogenic markers in the absence and presence of BMP-9

Quantitative RT-PCR normalized to day 0 of A) Sox9, B) Col2a1, C) ACAN, D) COMP, and E) Col10A1 in hMSCs on MC-GAG at 3, 7, and 14 days in the absence and presence of AdBMP-9 transduction.

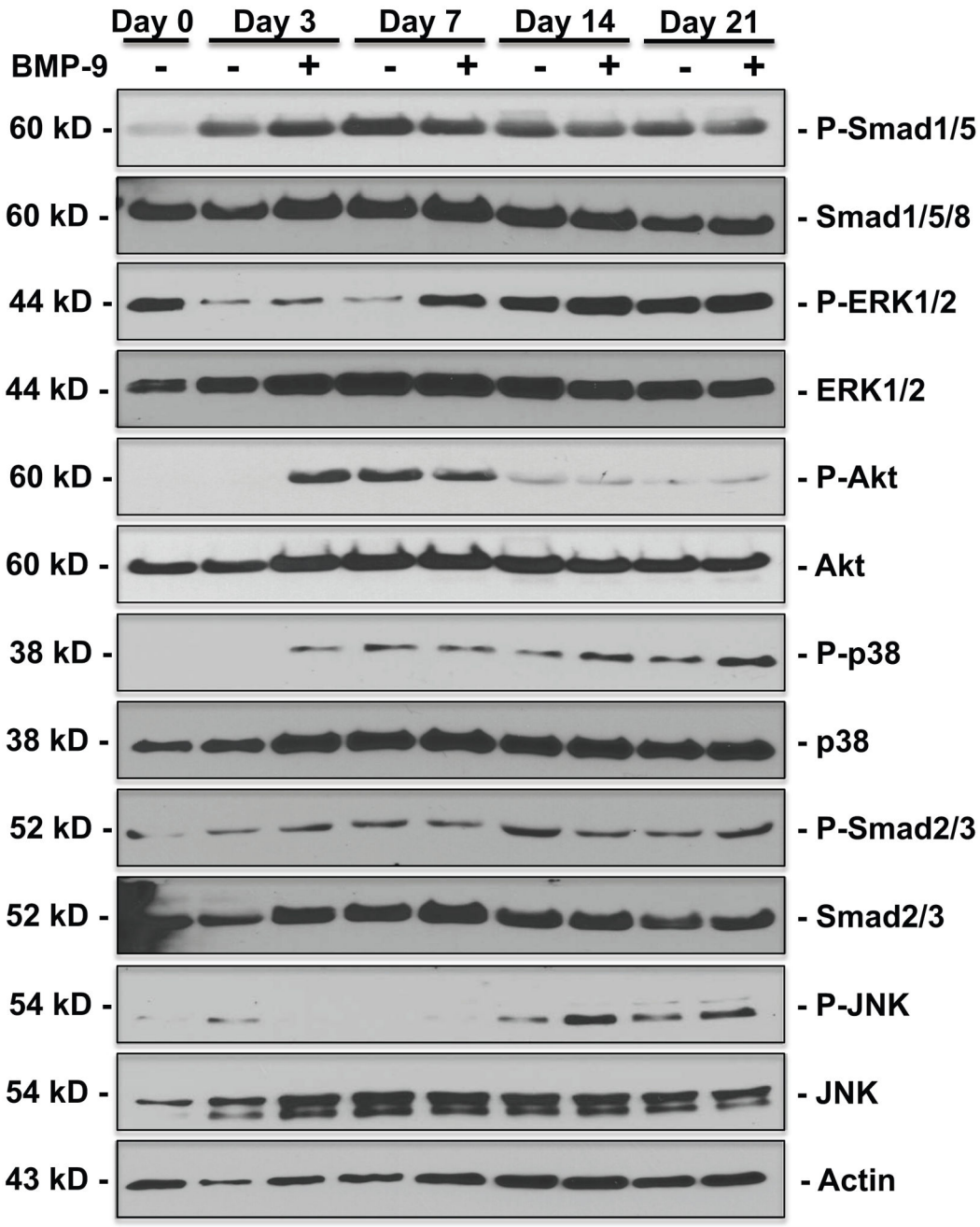

Figure 7. Differential activation of intracellular signaling molecules in the absence and presence of BMP-9

Western blots of p-Smad1/5, total Smad 1/5/8, p-ERK1/2, total ERK1/2, p-Akt, total Akt, p-p38, total p38, p-Smad2/3, total Smad 2/3, p-JNK, total JNK, and actin were performed in control and BMP-9 transduced hMSCs cultured on MC-GAG scaffolds for 0, 3, 7, 14, and 21 days.

Table 1

Primer Sequences

Genes	Oligonucleotide Sequence
18S sense	5′-CGGGTCATAAGCTTCGTT-3′
18S antisense	5′-CCGCAGGTTCACCTACGG-3′
β-Actin sense	5′-TCACCCACACTGTGCCCCATCTACGA-3′
β-Actin antisense	5′-CAGCGGAACCGCTCATTGCCAATGG-3′
ALP sense	5′-AAGCCGGTGCCTGGGTGGCCAT-3′
ALP antisense	5′-ACAGGAGAGTCGCTTCAGAG-3′
Col I sense	5′-TGCGACATGGACACTGGGGC-3′
Col I antisense	5′-GAGCCTTCGCTGCCGTACTCG-3′
OPN sense	5′-AGTCTGATGAGTCTGATGAAGTCAC-3′
OPN antisense	5′-GTGACTTTGGGTTTCCACGC-3′
BMP9 sense	5′-CGAAACACGCTATCGTGCAG-3′
BMP9 antisense	5′-CTACCTGCACCCACACTCTG-3′
COL2A1 sense	5′-GGGGAGAAGACGCAGAGC-3′
COL2A1 antisense	5′-GACATCCTGGCCCTGACAC-3′
SOX9 sense	5′-GAAGGACCACCCGGATTACA-3′
SOX9 antisense	5′-GGGAGATGTGCGTCTGCTC-3′
ACAN sense	5′-TGGTGATGATCTGGCACGAG-3′
ACAN antisense	5′-CTCCGCTTCTGTAGTCTGCG-3′
COMP sense	5′-CTTCAGGGCCTTCCAGACAG-3′
COMP antisense	5′-CGCATAGTCGTCATCCGTGA-3′
COL10A1 sense	5′-AACTCCCAGCACGCAGAATC- 3′
COL10A1 antisense	5′-GGACTTCCGTAGCCTGGTTT- 3′

ALP, alkaline phosphatase; Col I, type I collagen; OPN, Osteopontin; BMP, bone morphogenetic protein; COL2A1, type II collagen; ACAN, aggrecan; COMP, cartilage oligomeric matrix protein, COL10A1, type X collagen